MoDeNa

Authors:

Patrick Anderson
Javier Llorca
Juraj Kosek
Daniele Marchisio
Christos Mitrias
Pavel Ferkl
Mohammad Marvi Mashadi
Mohsen Karimi

Deliverable D3.5

Validation: Model validation and realistic ways of controlling the foam morphology on macro-scale

Principal investigators:

Patrick Anderson

Collaborators:

Juraj Kosek
Javier Llorca
Daniele Marchisio
Christos Mitrias
Pavel Ferkl
Mohammad Marvi Mashadi
Mohsen Karimi

Project coordinator:

Heinz A Preisig

heinz.preisig@chemeng.ntnu.no

Abstract:

This document elaborates Polito's contributions on D3.5 which is focused on the validation of the macro-scale tool for PU foam and describes the details of Task 3.5. Two dimensional validation tests were performed for two different cup geometries. Further material properties such as specific heat, thermal conductivity and density were included in Deliverable 3.4.

Contents

1 Part 1: Polito's contributions

D3.5 - Validation: Model validation and realistic ways of controlling the foam morphology on macro-scale

M. Karimi,
D. L. Marchisio

Department of Applied Science and Technology, Politecnico di Torino.

This document elaborates Polito's contributions on D3.5 which is focused on the validation of the macro-scale tool for PU foam.

Two dimensional validation tests are performed for two different geometries. The first one is a cup used in batch 1 to batch 11 with dimensions of 8.5 cm × 20 cm and the second geometry is 10 cm × 20 cm. To minimize the effect of numerical uncertainties due to the discretization of the domain, the typical grid independent study is conducted for both geometries and it was decided that a structured mesh of 34×80 elements for the first geometry and 20×40 elements for the second geometry should be utilized. It is worth indicating here that simulations are also performed on 2D planar, 2D axi-symmetric, wedge and 3D grids, however the results show trivial differences.

The first 10 % of the cups is filled with the liquid mixture (i.e., $\alpha_f = 1$) with a temperature of 298 K and the rest is filled with air. An atmospheric boundary condition is prescribed at the cups lids and the other faces are assumed to be walls, meaning zero gradient boundary conditions for the volume fraction, moments, temperature and kinetics related fields.

Preliminary tests are also carried out to analyze the influence of spatial and temporal discretization schemes. The analysis shows that the first-order implicit Euler scheme for the temporal derivative, the first-order upwind differencing scheme for the divergence term, and the standard Gauss linear method for the Laplacian and gradient terms should be applied to discretize the governing equations.

In order to evaluate the predictive potential of the developed model, experimental measurements from literature have been extracted and categorized into 12 different batches. The measurements include the temperature rise and the density fall with time of the simple PU foam expansion experiments conducted in a cylinder. In that, polyol, isocyanate, blowing agents and other additives are mixed inside a cylindrical cup and the expansion is monitored and recorded. The density measurements were performed based on the rising height of the foam as a function of time, whereas the experimental measurements of tem-

1

perature were conducted using a thermocouple at a certain height of the cup. The corresponding point is also selected in the computational domain when the comparison is done.

The main difference of various batches are the chemical recipes employed. Batch 1 to batch 11 used polyether polyol with OH value of 365 mg KOH/g polyol, and polymethyline-poly(phenyl isocyanate) with an equivalent molecular weight of 135. The recipe for batch 12 includes a mixture of different polyols with OH number of 370 and a mixture of MDI (methane diisocyanate) and TDI (toluene diisocyanate). R-11 (i.e., trichlorofluoromethane) was used as the physical blowing agent in batches 2 to 5 and batches 10 and 11, whereas the physical blowing agent used in batch 12 was n-pentane. It should be indicated that due to the absence of both physical and chemical blowing agents in batch 1 and batch 6 only polymerization, without foaming, is modeled. The initial concentrations of reactants for each batch is reported in Table 1. Moreover, the kinetics details are summarized in Table 2.

Table 1: Summary of the initial conditions of batches investigated. For all the batches the initial temperature was 298 K.

Batch	C_{OH}^0 $(\mathrm{mol\,m^{-3}})$	C_{NCO}^0 $(\mathrm{mol\,m^{-3}})$	C_W^0 $(\mathrm{mol\,m^{-3}})$	w_i^0 $(\mathrm{kg\,kg^{-1}})$
1	3700	3700	0	0
2	3700	3700	0	0.159
3	3700	3700	0	0.106
4	3700	3700	0	0.131
5	3700	3700	0	0.057
6	4400	4400	0	0
7	4400	4400	305	0
8	4400	4400	610	0
9	4400	4400	915	0
10	4400	4400	915	0.050
11	4400	4400	305	0.135
12	5140	4455	671	0.057

For the batches investigated, the initial BSD cannot be experimentally measured with high accuracy. Thus, for all the test cases the first four moments of the BSD are initialized to those of a log-normal distribution with mean and variance approximately equal to 1 μm and 0.1, respectively, in line with qualitative experimental information. The initial values of moments are therefore: $m_0 = 1.00 \times 10^{13}$ (m^{-3}), $m_1 = 5.26 \times 10^{-6}$, $m_2 = 2.80 \times 10^{-24}$ (m^{-3}), and $m_3 = 1.50 \times 10^{-42}$ (m^6).

The model constants that have been applied within the solver, are also summarized in Table 3.

Before validating model predictions with experiments, let us analyze the results of batch 2 and batch 9 (see Table. 1). Batch 2 represents a physically-

Table 2: Summary of the kinetics parameters.

Batch	A_{OH} $\mathrm{m^3\,mol^{-1}\,s^{-1}}$	E_{OH} $\mathrm{J\,mol^{-1}}$	$-\Delta H_{\mathrm{OH}}$ $\mathrm{J\,mol^{-1}\,K^{-1}}$	A_{W} $\mathrm{s^{-1}}$	E_{W} $\mathrm{J\,mol^{-1}}$	$-\Delta H_{\mathrm{W}}$ $\mathrm{J\,mol^{-1}}$
1-5	1965	5.49×10^4	7.49×10^4	-	-	-
6-11	1.735	4.04×10^4	7.07×10^4	1390	3.27×10^4	8.60×10^4
12	1.0	3.15×10^4	6.85×10^4	1050	2.70×10^4	8.15×10^4

Table 3: Summary of model constants applied in the solver.

Property	Value
c_{f}	1800 ($\mathrm{J\,kg^{-1}\,K^{-1}}$)
$M_{\mathrm{CO_2}}$	44.0 ($\mathrm{kg\,kmol^{-1}}$)
M_{R11}	137.37 ($\mathrm{kg\,kmol^{-1}}$)
$M_{\mathrm{n\text{-}pentane}}$	72.15 ($\mathrm{kg\,kmol^{-1}}$)
M_{NCO}	615.0 ($\mathrm{kg\,kmol^{-1}}$)
P	1.0×10^5 (Pa)
R	8.314 ($\mathrm{J\,mol^{-1}\,K^{-1}}$)
Λ	2.0×10^5 ($\mathrm{J\,kg^{-1}}$)
ρ_{a}	1.2 ($\mathrm{kg\,m^{-3}}$)
ρ_{PU}	1100 ($\mathrm{kg\,m^{-3}}$)

blown PU foam with the highest weight fraction of blowing agent, whereas the expansion of PU foam in batch 9 is solely due to the presence of water (i.e., chemically-blown foam). The idea is to assess the solver stability under two divergent circumstances, when the foam expands either due to evaporation or blowing reaction. Figure 1 shows the expansion of the foam in terms of the volume fraction of the surrounding gas as a function of time. Four time instants have been selected to represent the interface. The initial volume fraction of the foam phase is identical at the beginning ($t = 0$ s). After 15 seconds, the evaporation of physical blowing agent in batch 2 has set off the expansion, while the carbon dioxide in batch 9 has not reached to its equilibrium value yet. The production of CO_2 has, however, started at 45 seconds of simulation time, corresponding to the expansion seen in the figure. The large presence of the physical blowing agent clearly yields faster expansion, since after 90 seconds the cup for batch 2 is fully filled with the foam, while the computational domain for batch 9 has still cells with volume fraction of gas equal to unity. Furthermore, Figure 2 shows the conversion of hydroxyl groups at different time instants of the foaming process. As seen the kinetics of reaction is faster in the case of physically-blown foam and after 15 second the value of X_{OH} in the foam phase is approximately 0.1, while the reaction has not started in batch 9. The conversion of OH continuously progresses and after 45 seconds in batch 2 it is close to its final value, while for the chemically blown foam the conversion is at the beginning ($X_{\mathrm{OH}} = 0.1$) and at the last time instant the maximum value of
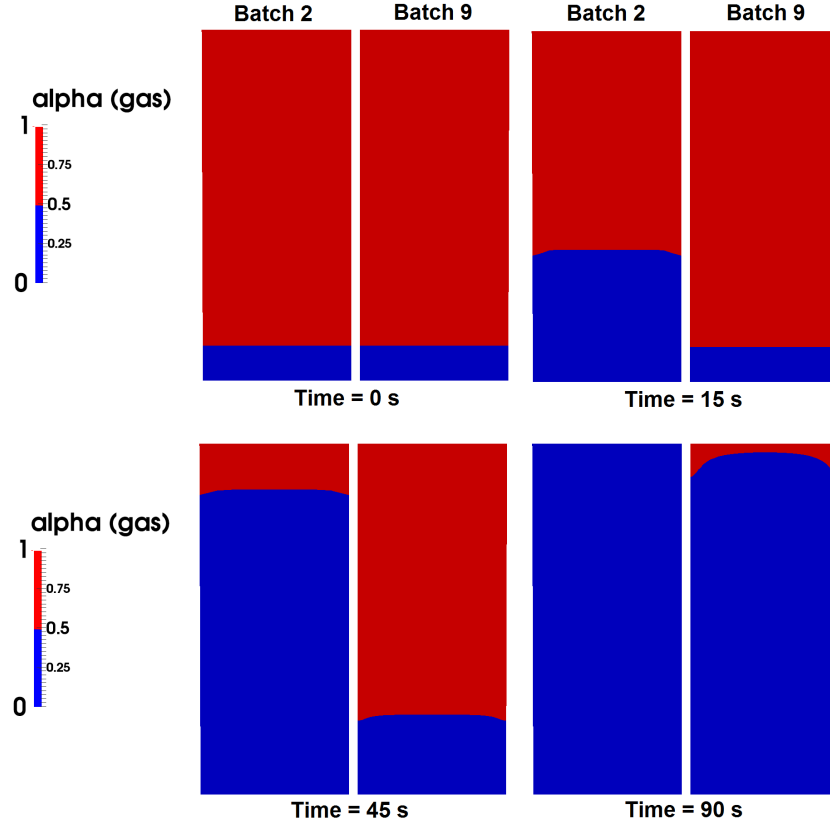
Figure 1: Comparison of the gas volume fraction at different simulation times for physically-blown (batch 2: $C_W^0 = 0$ mol m^{-3}, $w_{R11}^0 = 0.159$ kg kg^{-1}) and chemically-blown (batch 9: $C_W^0 = 915$ mol m^{-3}, $w_{R11}^0 = 0$ kg kg^{-1}) foams.

conversion for batch 9 is approximately 36% less than the corresponding value in batch 2. It is important to stress here that, thank to the optimization work done on the solver, no stability issues were encountered for these two extreme cases, as well as the overall mass conservation was respected with errors smaller than 5 %.

Figure 3 compares the time variations of foam density (continuous lines), predicted numerically, with the experimental measurements (symbols). Since batch 1 and batch 6 includes only polymerization (i.e., no blowing agents in the recipes), they are excluded from this figure. Further, for batch 3 only temperature measurements are available. The results show that in all the test cases the decreasing profile of density has been captured correctly. In that, the density starts to decrease from the value of liquid mixture density and after a sharp drop, it eventually leans toward its final value. The flat line observed is associated with the required time for the blowing agents (either chemical or physical) to reach
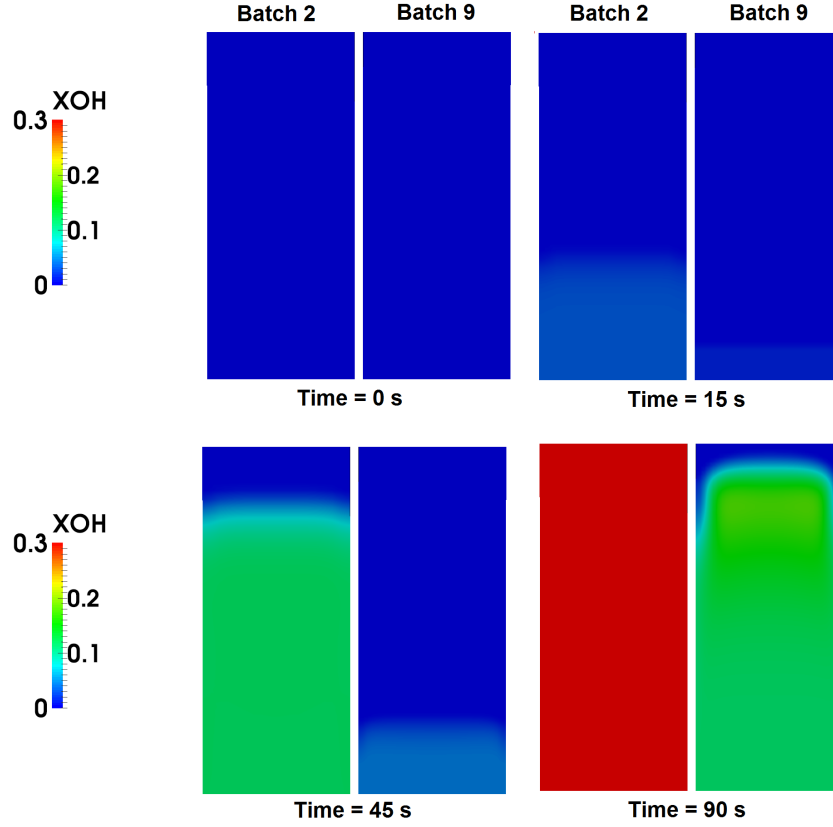
Figure 2: Comparison of the conversion of hydroxyl groups at different simulation times for physically-blown (batch 2: $C_W^0 = 0$ mol m^{-3}, $w_{R11}^0 = 0.159$ kg kg^{-1}) and chemically-blown (batch 9: $C_W^0 = 915$ mol m^{-3}, $w_{R11}^0 = 0$ kg kg^{-1}) foams.

to the equilibrium values. In other words, the temperature of the polymerizing mixture continuously increases due to the exothermic reactions. Once a critical temperature is reached, the amount of blowing agent in the liquid is greater than maximum soluble amount of blowing agent. Thus, the evaporation of blowing agents begins and the bubbles start to grow leading to the decrease of the foam density. In the chemically blown batches (i.e., batch 7 to batch 9), the shorter times to obtain the critical temperature can be attributed to the small value for the solubility of carbon dioxide (equals to 4.4×10^{-4}). As stated, this simplification will be improved in the near future. It is worth noting that the density of final product for the physically blown foams (batch 2 to batch 5) increases by decreasing the amount of blowing agent, and the same pattern is observed when the PU foam is solely blown with the chemical blowing agent (batch 7 to batch 9). This implies that by relating the foam density to the volume of bub-

bles the solver is able to directly link three crucial physical phenomenon during the foaming, chemical reactions, evaporation of blowing agents and the bubble growth, and in return it converges their effects into the foam density. Figure 4
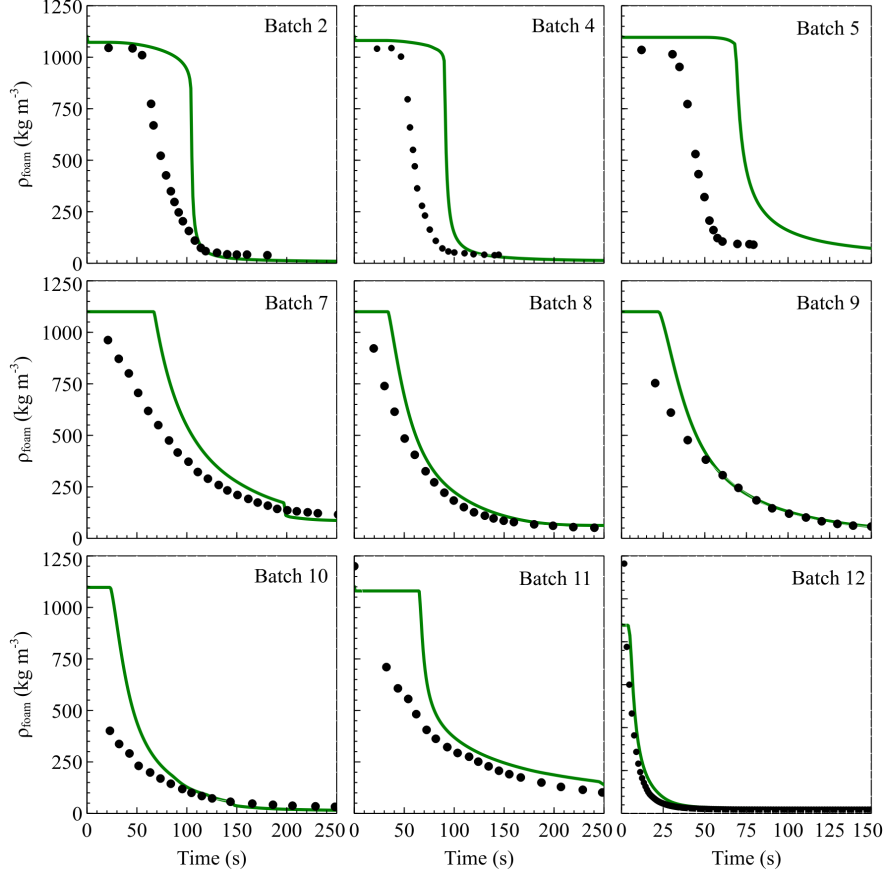

Figure 3: The time evolution of foam density predicted by the developed solver (continuous line) compared with the experimental measurements (symbols) for the test cases considered.

shows the numerical predictions of temperature (continuous line) in comparison with the experimental data (symbols). The overall qualitative level of agreement between the predictions and experiments shows the solver potential for simulating the temperature rise during the foaming process. Comparison of the temperature profile between physically blown batches (batch 2 to batch 5) with chemically blown batches (batch 7 to batch 9) shows that the final temperature for the physically blown foam is generally lower than that of chemically blown foams. For example at the highest amount of physical blowing agent (batch 2, $w_{R11}^0 = 0.159$ kg kg^{-1}) the final predicted temperature reaches to 402 K,

whereas in batch 9 with the highest amount of water ($C_0^W = 915$ mol m^{-3}) the final temperature is 430 K. This is indeed related to the consumption of heat during the evaporation of physical blowing agent and the heat of blowing reaction is the main reason for batch 7 to batch 9 to have higher temperature at the end of expansion. However, in batch 10 to batch 12 (physically and chemically blown foams) the competition between exothermic and endothermic reactions quantifies the final temperature. It should be pointed out that the simulations are performed under adiabatic condition (i.e., no heat transfer between the cup and its surrounding) and hence the temperature decrease because of external cooling is not explained (see batch 12 in Figure 4).

In order to investigate how the presence of blowing agents influence the mean bubble diameter hroughout the foam expansion, Figure 5 shows a comparison of the mean bubble diameter predictions for the physically and chemically blown foams at different initial amounts of blowing agents. As expected, the solver results demonstrate a continuous increase in the bubble diameters. Increasing the amount of blowing agent (either chemical or physical) increases the amount of gas within the mixture causing further bubble enlargement. Moreover, the initial time that is needed for the temperature to rise and trigger the evaporation of the blowing agents is reflected by the time delay (flat line) at the beginning of the plots. This time is usually shorter for the chemically blown foams due to the small value adopted for the solubility of carbon dioxide and for the relatively fast blowing reaction. Finally, to emphasize on the influence of the physical blowing agent, one can observe that the purely physically-blown foams produce bubbles whose final mean diameter is larger than that of the chemically-blowing foams, conclusion in line with experimental observations.
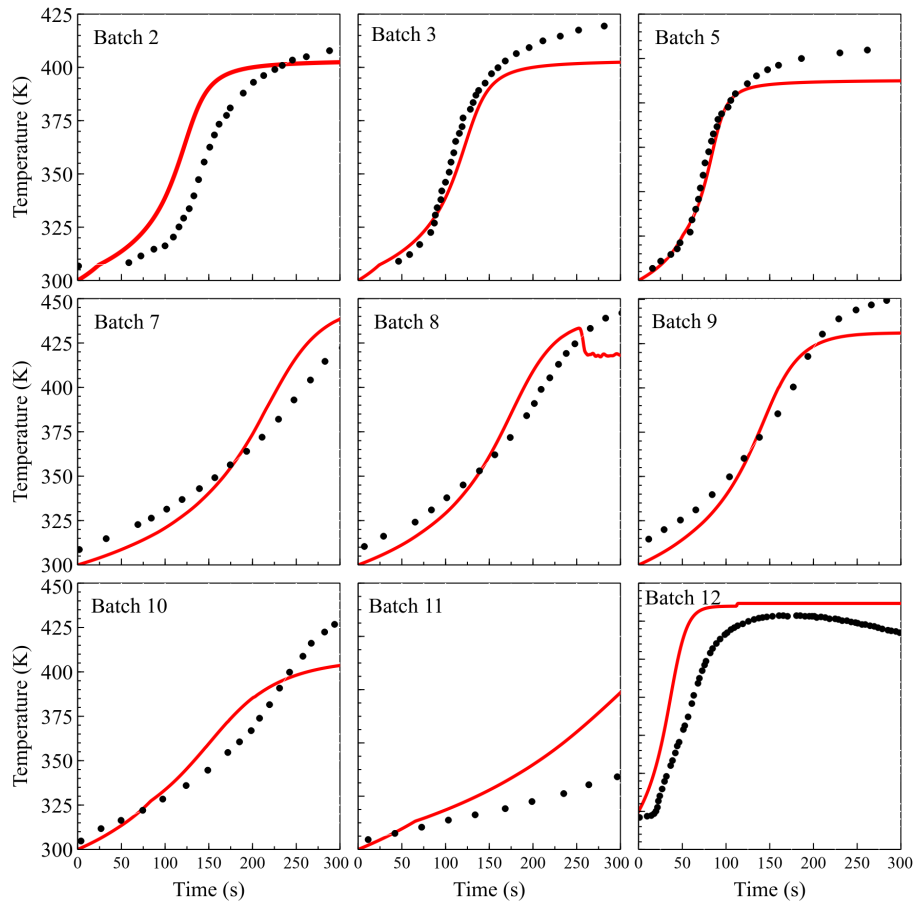
Figure 4: The time evolution of foam temperature predicted by the solver (continuous line) compared with the experimental measurements (symbols) for the test cases considered.
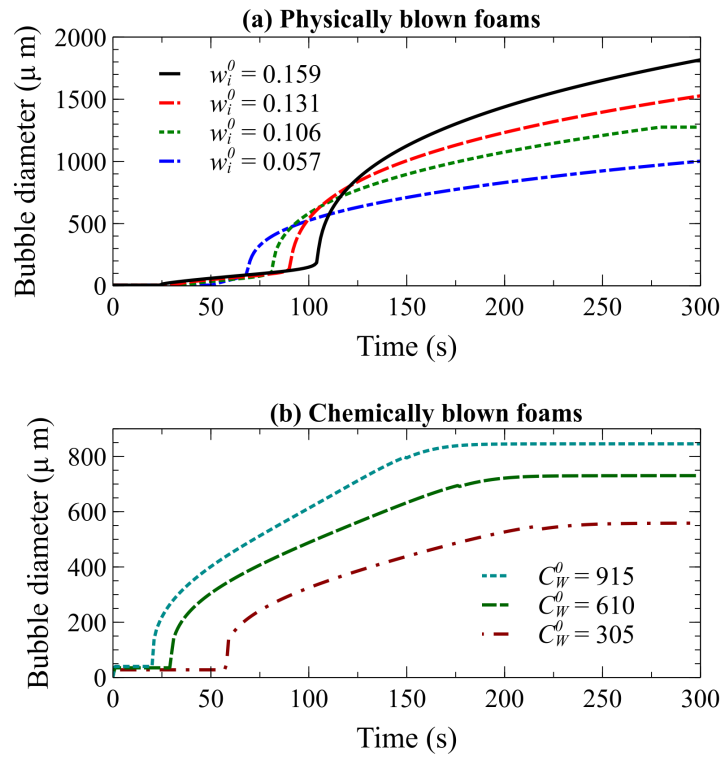
Figure 5: Time evolution of the mean bubble diameters for (a) physically blown foams corresponding to batch 2 to batch 5 and (b) chemically blown foams corresponding to batch 7 to batch 9.